Research Article | Vol. 26, No. 23 | 12 Nov 2018 | OPTICS EXPRESS 30108

Optics EXPRESS

High-sensitivity gas pressure sensor based on hollow-core photonic bandgap fiber Mach-Zehnder interferometer

CHUN MAO, BO HUANG, YING WANG*, YIJIAN HUANG, LONGFEI ZHANG, YU SHAO, AND YIPING WANG

Key Laboratory of Optoelectronic Devices and Systems of Ministry of Education and Guangdong Province, College of Optoelectronic Engineering, Shenzhen University, Shenzhen 518060, China
*yingwang@szu.edu.cn

Abstract: We propose and experimentally demonstrate a highly sensitive gas pressure sensor based on a near-balanced Mach-Zehnder interferometer (MZI) and constructed by hollow-core photonic bandgap fiber (HC-PBF) in this paper. The MZI is simply constructed by fusion splicing two HC-PBFs, which are of slightly different lengths, between two 3-dB couplers. The two output ends of each coupler are approximately equal in length, to ensure that the optical path variations of the MZI only result from the differences in the lengths between the two HC-PBFs. To apply the MZI for gas pressure sensing, a femtosecond laser is employed to drill a micro-channel in one of the two HC-PBF arms. The experiment result shows that the proposed MZI based gas pressure sensor achieves an ultrahigh sensitivity, up to 2.39 nm/kPa, which is two orders of magnitude higher than that of the previously reported MZI-based gas pressure sensors. Additionally, the effects resulting from the absolute length and relative length of the two HC-PBFs on gas pressure sensing performance are also investigated experimentally and theoretically, respectively. The ultra-high sensitivity and ease of fabrication make this device suitable for gas pressure sensing in the field of industrial and environmental safety monitoring.

1. Introduction

Gas pressure sensors are one of the most widely used sensors for industrial and environmental monitoring. With the advantages of immunity to electromagnetic interference, fast signal acquisition, high sensitivity and compact structure, optical fiber sensors have been extensively investigated for gas pressure sensing. A variety of optical fiber pressure sensors based on various types of fiber components, including long-period fiber gratings (LPFGs) [1–6], fiber Bragg gratings (FBGs) [7–11], and fiber interferometers [12–26] have been proposed in recent years. LPFGs inscribed in single-mode fiber (SMF) [1], photonic crystal fiber [2–4], polymer micro-structured fiber [5], boron co-doped optical fiber [6] and FBGs inscribed in single-mode fiber [7,8], side-hole fiber [9], air-hole micro-structured fiber [10,11], have been used as gas pressure sensors, respectively. However, the maximum sensitivity of abovementioned fiber gratings based gas pressure sensors is only 1.68 pm/kPa [3], which is relatively low. The fiber interferometers based gas pressure sensors, by contrast, are attractive due to their high sensitivity. Fabry-Perot interferometers (FPIs) constructed with different fibers including hollow-core micro-structured fibers [12,13] and capillaries [14,15] have been proposed as gas pressure sensors, or various diaphragm materials, such as silica [16–19], polymers [20,21], silver [22,23], and graphene [24], have been employed as sensitive films to construct diaphragm-based FPIs to achieve high sensitivity in gas pressure measurement. And the silver diaphragm based FPI [23] has exhibited an ultrahigh gas pressure sensitivity of 70.5 nm/kPa in forms of cavity length variation, however, the poor mechanical property makes it unsuitable for high pressure sensing. Mach-Zehnder interferometer (MZI) has also been

#346039 https://doi.org/10.1364/OE.26.030108
Journal © 2018 Received 20 Sep 2018; revised 18 Oct 2018; accepted 25 Oct 2018; published 31 Oct 2018

Optics EXPRESS

employed as gas pressure sensor. The fiber in-line MZIs based on an inner air-cavity with open micro-channel [25] and twin-core fiber [26] have been demonstrated for gas pressure sensing with the sensitivity of 8.239 pm/kPa and −9.6 pm/kPa, respectively. Overall, the sensitivity of the MZI based gas pressure sensor is relatively low, which needs to be further improved.

In this paper, we propose a highly sensitive MZI based gas pressure sensor, which is simply formed by fusion splicing two hollow-core photonic bandgap fibers (HC-PBFs) with different lengths between the equal-length output ports of two 3 dB couplers, respectively. To apply the MZI for gas pressure sensing, a femtosecond (fs) laser is employed to drill a micro-channel in one of the two HC-PBF arms. The arm lengths of the output ends are standardized in the two couplers to ensure that the optical path variations of the MZI are only resulted from differences in the lengths between the two HC-PBFs, thereby optimizing the sensitivity. The experimental results show that the proposed MZI based gas pressure sensor achieves a high sensitivity of 2.39 nm/kPa at ~1550 nm, which is two orders of magnitude higher than that of the previously reported MZI based gas pressure sensors. In addition, the effects resulting from the absolute length and relative length of the two HC-PBFs on gas pressure sensing performance are also investigated experimentally and theoretically, respectively. The high sensitivity and ease of fabrication make this device suitable for gas pressure sensing in the field of industrial and environmental safety monitoring.

2. Principle and device fabrication

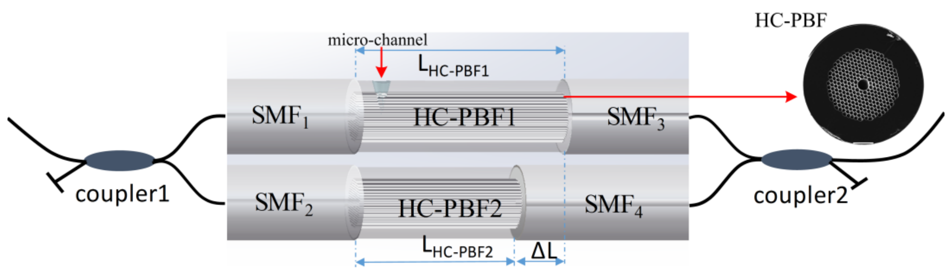

Fig. 1. Schematic diagram of the proposed HC-PBF-based MZI for gas pressure sensing.

Figure 1 shows the schematic diagram of the proposed HC-PBF-based MZI for gas pressure sensing. The HC-PBF used in the experiment is a commercial HC-1550-02 PBF from NKT photonics and a scanning electron microscope (SEM) micrograph of the fiber cross-section is shown in the upper-right inset of Fig. 1. The hollow-core with a diameter of 10 μm is surrounded by an air/silica microstructure cladding and a pure silica cladding. The air/silica holey lattice exhibits an average pitch value of 3.8 μm, the thickness of the silica walls between cladding-holes is about 0.34 μm, and the air-filling ratio of the holey lattice is above 90%. The diameters of the holey cladding and fiber are 70 μm and 120μm, respectively. The two HC-PBFs with different lengths $L_{HC\text{-}PBF1}$ and $L_{HC\text{-}PBF2}$ are fusion spliced between two 3-dB couplers. The two output ends of each coupler are equal in length (i.e., $L_{SMF1} = L_{SMF2}$ and $L_{SMF3} = L_{SMF4}$) and a micro-channel is drilled on one of the two HC-PBFs using fs laser micromachining. The working principle of the proposed MZI can be described as follows: the light propagating through coupler1 is equally split into two beams propagating along the two arms of the MZI, respectively. And then, an optical path difference (OPD) between the two beams is induced by the difference ΔL in the lengths between the two HC-PBFs. Finally the two beams meet at coupler2 and the interference occurs.

The fabrication process of the proposed MZI based gas pressure sensor involves three steps. In the first step, the two outputs of each 3-dB couplers are cut to be approximately equal lengths using a precision cutting device (SUN Way Industrial Camera, FC-6S Cleaver). As we know, for the 3-dB coupler with length difference between the two arms, the

Optics EXPRESS

Michelson interference spectrum can be observed in the reflected spectrum. So, according to the free spectral range (FSR) of the interference spectrum, the length difference between the two arms can be calculated. In the experiment, the two arms are assumed to be equal in length when the FSR of the reflection spectrum is beyond 160 nm, which corresponds to an arm-length-difference of less than 5 μm. In the second step, the two HC-PBFs with different lengths ($\Delta L = L_{HC\text{-}PBF1}\text{-}L_{HC\text{-}PBF2}$) are fusion spliced with the two couplers, respectively, by using a commercial fusion splicer (FSM-60) in manual mode. During the splicing of the HC-PBF, the end facet of PBF must be kept away from the central area of the electrode to prevent the excessive discharge and collapse of the air holes. Non-ideal fusion splicing may excite higher order modes and result in multi-mode interferences, which will degrade the resolution and accuracy of the device. To achieve good welding results in the experiment, the parameters including the arc time, arc power, and overlap distance are optimized. In the third step, a side-opened micro-channel is drilled in one of the HC-FBFs by using an fs laser (Spectra-Physics Solstice, 120 Fs, 800 nm, 1 kHz, 4 mJ). The detailed process can be described as follows: one of the HC-PBF arms is mounted on a computer-controlled three-axis translation stage with a resolution of 10 nm. The fs laser beam with a pulse energy of 7 μJ is then focused onto the top surface of the HC-PBF using an objective lens with an NA value of 0.25. By controlling the translation stage to move the HC-PBF in the opposite direction to the laser beam, a micro-channel can be created.

3. Gas pressure sensing experiment and results

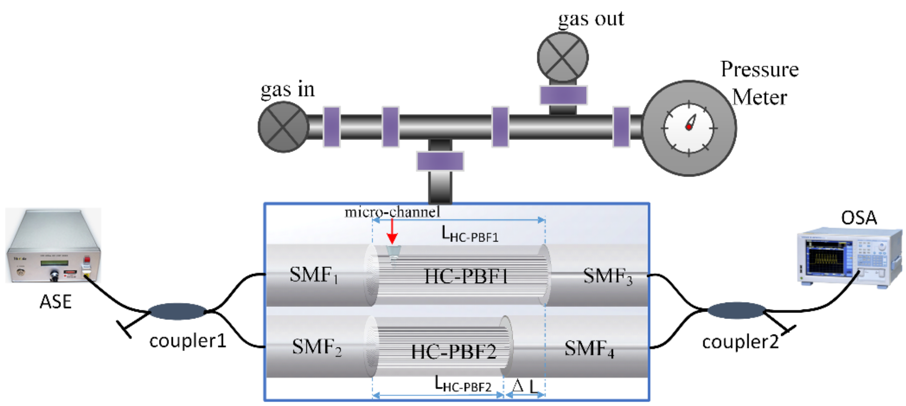

Fig. 2. Schematic diagram of the experimental setup for gas pressure sensing measurement

The gas pressure response of the proposed sensor is investigated via the experimental setup shown in Fig. 2. The sensor sample is placed into an air chamber controlled by a commercial gas pressure generator with a stability of ± 0.2 kPa. A high-precision digital gas pressure gauge (ConST-811) is employed to measure the gas pressure inside the chamber. Both ends of the chamber are sealed with a strong glue. To monitor the interference spectrum in real-time, a broadband light source (Fiber Lake, ASE) with a wavelength range from 1250 to 1650 nm and an optical spectrum analyzer (OSA, YOKOGAWA AQ6370C) with a resolution of 0.05 nm are connected to the input port and output port of the MZI, respectively. And then, the gas pressure test are carried out by increasing the gas pressure of the air chamber from 5 to 35 kPa. Chamber pressure is increased with an increment of 5 kPa and maintains for 5 minutes, and then the corresponding transmission spectra of the sensor is recorded by OSA.

Optics EXPRESS

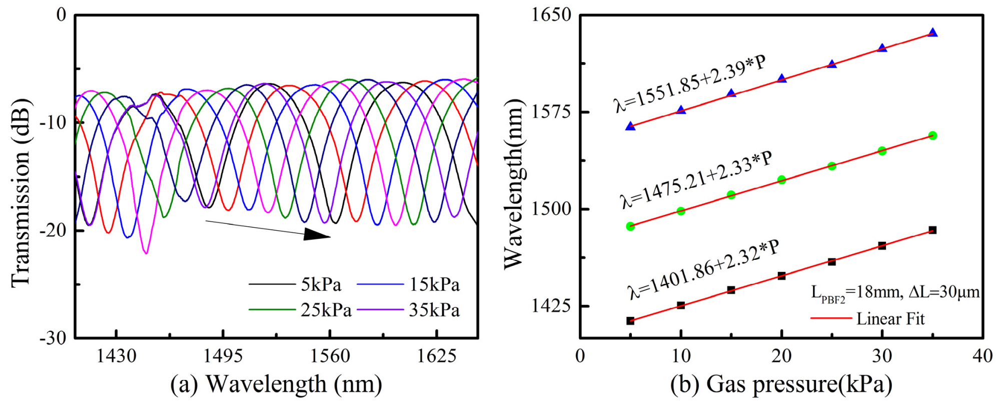

Fig. 3. (a) The transmission spectrum variations and (b) the pressure response of of the MZI with $L_{HC\text{-}PBF2}$ = 18 mm and ΔL = 30 µm.

Figure 3(a) shows the transmission spectra of the sensor with $L_{HC\text{-}PBF2}$ = 18 mm and ΔL = 30 µm under different gas pressures at room temperature. And the micro-channel drilled by fs laser is on HC-PBF1. Three dips at ~1401 nm, ~1475 nm and ~1551nm are tracked within the scanning wavelength ranging from 1400 to 1650 nm. It can be seen clearly that with the increase of the gas pressure, the dips shift towards longer wavelengths. The relationship between the gas pressure and the wavelengths of the three dips is demonstrated in Fig. 3(b), where we can observe that the wavelengths of the three dips change linearly with the gas pressure. Through linear fitting, we get the gas pressure sensitivities of 2.32 nm/kPa, 2.33 nm/kPa and 2.39 nm/kPa for these interference dips, respectively, which are two orders of magnitude higher than that of the previously reported MZI based gas pressure sensors [25,26].

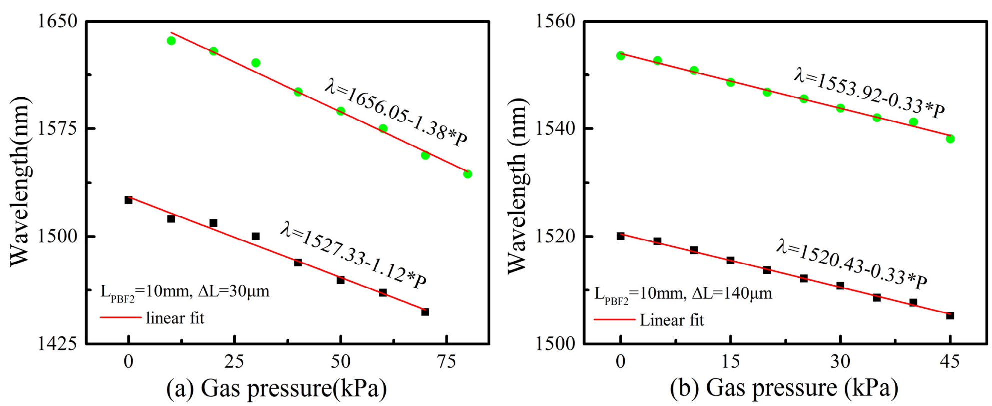

Fig. 4. Relationship between gas pressure and the dip wavelengths for MZIs with $L_{HC\text{-}PBF2}$ = 10 mm in case of (a) ΔL = 30 µm and (b) ΔL = 140 µm.

To investigate the influence of the relative length, namely the length difference ΔL of two HC-PBFs, on gas pressure sensitivity, two MZI based sensors with $L_{HC\text{-}PBF2}$ = 10 mm, ΔL = 30 µm, and $L_{HC\text{-}PBF2}$ = 10 mm, ΔL = 140 µm are used for testing the pressure response. For each sensor employed in the test, the micro-channel is drilled on HC-PBF2. Figure 4 shows the relationship between the dip wavelengths and gas pressure. For the two sensors with ΔL = 30 µm, and ΔL = 140 µm, the achieved pressure sensitivities are −1.12 nm/kPa and −0.33 nm/kPa for the dips at the wavelength of ~1550 nm, respectively, indicating that the gas pressure sensitivity decreases with the relative length ΔL increasing.

Optics EXPRESS

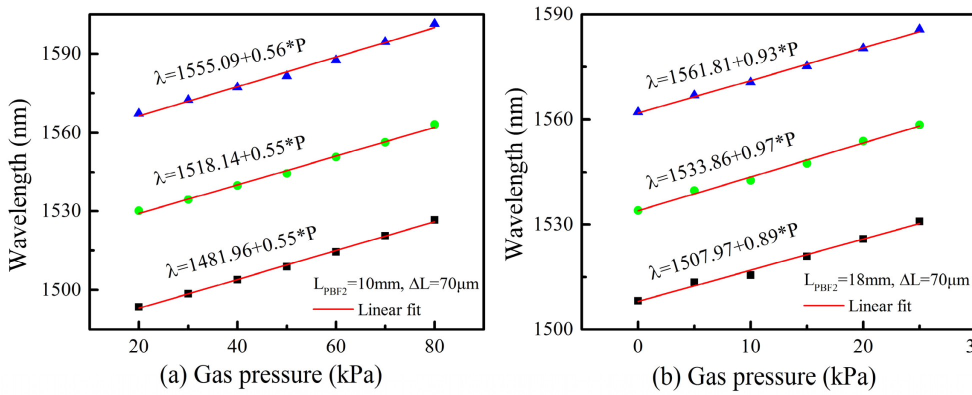

Fig. 5. The relationship between gas pressure and the dip wavelengths for MZIs with ΔL = 70 μm in case of (a) $L_{HC\text{-}PBF2}$ = 10 mm and (b) $L_{HC\text{-}PBF2}$ = 18 mm.

Then, the influence of the absolute length $L_{HC\text{-}PBF2}$ on gas pressure sensitivity is also investigated. Figures 5(a) and 5(b) depict the relationship between dip wavelength and gas pressure for the two HC-PBF-based MZIs with ΔL = 70 μm, $L_{HC\text{-}PBF2}$ = 10 mm, and ΔL = 70 μm, $L_{HC\text{-}PBF2}$ = 18 mm, respectively. The pressure sensitivity for the dip at around 1550 nm is calculated to be 0.55 nm/kPa and 0.97 nm/kPa, respectively. The obtained experimental results indicate that a higher gas pressure sensitivity can be achieved simply by increasing the absolute length of HC-PBFs.

In addition, it is worthy noting that the shift directions of the transmission spectra are not the same in the previous experiments, as can be seen clearly in Figs. 3-5. Actually, for the sensor with the micro-channel drilled on the longer PBF (HC-PBF1), the transmission spectrum exhibits a red shift with the increase of gas pressure. Conversely, the transmission spectrum experiences a blue shift as the gas pressure increased, when the micro-channel is drilled in the shorter PBF (HC-PBF2). The mechanism will be discussed in the next section.

4. Analysis and discussion

The ultrahigh gas pressure sensitivity of the proposed sensor is mainly originated from the near-balance design of the MZI, where the contribution of pressure induced fiber length change to gas pressure sensitivity can be ignored due to the large Young's modulus of silica. The output intensity of the HC-PBF-based MZI with the micro-channel drilled on HC-PBF1 can be expressed as:

$$I = I_1 + I_2 + 2\sqrt{I_1 I_2}\cos\left(\frac{2\pi\left(nL_{HC-PBF1} - n_0 L_{HC-PBF2}\right)}{\lambda} + \varphi_0\right), \tag{1}$$

where λ is the wavelength in vacuum, $L_{HC\text{-}PBF1}$ is the length of longer HC-PBF, $L_{HC\text{-}PBF2}$ is the length of shorter HC-PBF, ΔL is the length difference between the two HC-PBFs, n and n_0 are the refractive indices (RIs) of air in the hollow core after pressurization and under normal pressure, respectively, and φ_0 is the initial phase of the interference.

According to Eq. (1), the interference signal reaches the minimum value when the following condition is satisfied:

$$\frac{2\pi\left(nL_{HC-PBF1} - n_0 L_{HC-PBF2}\right)}{\lambda_m} + \varphi_0 = (2m+1)\pi, \tag{2}$$

where m is an integer and λ_m is the wavelength of the m^{th} order interference dip.

For the proposed sensor with a micro-channel drilled on HC-PBF1, the gas pressure sensitivity can be derived from Eq. (2) as:

Optics EXPRESS

$$\frac{d\lambda}{dP}=\frac{\lambda}{n-\frac{L_{HC-PBF2}}{L_{HC-PBF2}+\Delta L}n_0}\frac{dn}{dP}, \tag{3}$$

where dn/dP represents the RI variation of air in HC-PBF1 induced by pressure. At room temperature (15–25 °C), the RI of air is a function of the pressure and temperature [27]:

$$n=1+\frac{2.8793\times10^{-9}\times P}{1+0.003671\times t}, \tag{4}$$

where n, P and t are the RI of air, the gas pressure (in Pa), and the temperature (°C), respectively. The gas pressure induced RI variation of air dn/dP is calculated to be 2.63 × 10^{-6}/kPa at the temperature of 25 °C. From Eq. (3), we can know that when the relative length ΔL is a constant, the sensitivity $d\lambda/dP$ of the proposed gas pressure sensor increases with the absolute length $L_{HC\text{-}PBF2}$, which agrees well with the experiment results shown in Fig. 5. Considering that $n>n_0$, $L_{HC\text{-}PBF1}> L_{HC\text{-}PBF2}$ and $dn/dP>0$, the value of the sensitivity $d\lambda/dP$ is positive, which means that the interference dip shift to longer wavelengths with the gas pressure increasing. So we can see a red shift of the interference dip wavelength in the transmission spectrum of the sensor with a micro-channel drilled on HC-PBF1.

According to Eqs. (3) and (4), the sensitivity $d\lambda/dP$ is dependent on the gas pressure P. More specifically, the value of the sensitivity $d\lambda/dP$ slowly decreases as the gas pressure P increases. For the sensor with $L_{HC\text{-}PBF2}$ = 18 mm, ΔL = 30 μm and a micro-channel drilled on HC-PBF1, the calculated gas pressure sensitivities at ~1550nm are 2.23 nm/kPa and 2.43 nm/kPa under the gas pressure of 5 kPa and 35 kPa at the temperature of 25 °C. In view of that the measured gas pressure sensitivity 2.39 nm/kPa shown in Fig. 3(b) is a linear fitting value and is in the range of the calculated value, we can conclude that the experiment result is in consistence with the theoretical calculated result.

Similarly, for the proposed sensor with a micro-channel drilled on HC-PBF2, the pressure sensitivity can be expressed as:

$$\frac{d\lambda}{dP}=-\frac{\lambda}{(n_0-n)+\frac{\Delta L}{L_{HC-PBF2}}n_0}\frac{dn}{dP}. \tag{5}$$

In case of $n_0L_{HC-PBF1}-nL_{HC-PBF2}>0$, the value of $d\lambda/dP$ is negative, corresponding to a blue shift of the interference spectrum. When $L_{HC\text{-}PBF2}$ is a constant, the absolute value of $d\lambda/dP$ decreases with ΔL increasing, indicating that the gas pressure sensitivity decreases with ΔL increasing. On the other hand, in the case of $n_0L_{HC-PBF1}-nL_{HC-PBF2}<0$, the value of $d\lambda/dP$ is positive, corresponding to the red shift of the interference spectrum. For the two sensors with $L_{HC\text{-}PBF2}$ = 10 mm, ΔL = 30 μm, and $L_{HC\text{-}PBF2}$ = 10 mm, ΔL = 140 μm, they satisfy the condition of $n_0L_{HC-PBF1}-nL_{HC-PBF2}>0$, and the obtained experiment results shown in Fig. 4 agree well with the corresponding theoretical results.

The previous discussions are based on the assumption that the length of SMF1 is equal to that of SMF2, however, if they are not equal, then the sensitivity of the sensor will be reduced. For clarify, the arm-length-difference brought by two 3-dB coupler is nominated as ΔL′. Simulations on the influence of ΔL′ vs. pressure sensitivity have been carried out and the obtained results are shown in Fig. 6, where one can see clearly that the pressure sensitivity reduces dramatically from 2.43 nm/kPa to 1.33 nm/kPa with ΔL′ increasing from 0 to 25 μm for a device with HC-PBF length of 18 mm and ΔL of 30 μm. So to achieve pressure sensitivities as high as possible, it is necessary to ensure the two output port of 3-dB couplers are equal in length as far as possible in the experiment.

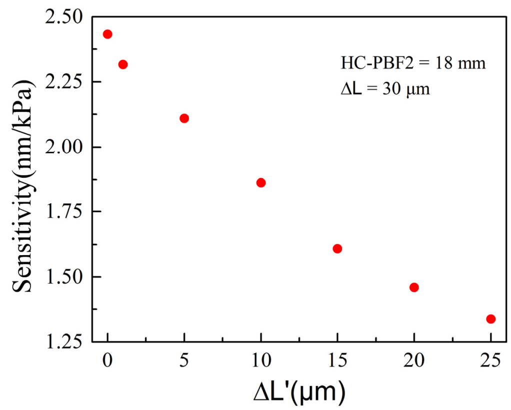

Fig. 6. The simulated pressure sensitivity of the sensor under different arm-length-difference (ΔL′) brought by two 3-dB coupler in the MZI.

5. Conclusion

A high sensitivity gas pressure sensor based on a HC-PBF MZI with near-balanced arms has been proposed and experimentally demonstrated in this paper. The proposed fiber MZI is simply fabricated by fusion splicing two HC-PBFs with different lengths between two 3-dB couplers with equal lengths at the output ports. For gas pressure sensing, a micro-channel is drilled in one of the two HC-PBFs using fs laser micromachining. Experimental results show that the sensitivity of the proposed gas pressure sensor is as high as 2.39 nm/kPa, which is two orders of magnitude higher than that of previously reported fiber MZI based gas pressure sensors. Additionally, the effects of absolute lengths of the two HC-PBFs and their relative length on gas pressure sensing performance are also investigated both in experiments and theoretical estimations. The ultra-high sensitivity and ease of fabrication make this device promising for gas pressure sensing in the field of industrial and environmental safety monitoring.

Funding

National Natural Science Foundation of China (NSFC) (61675137, 61425007, 61635007); Guangdong Natural Science Foundation (2015B010105007, 2014A030308007,2018A030310581); Science and Technology Innovation Commission of Shenzhen (JCYJ20170818093743767, JCYJ20160427104925452, JCYJ20170412105604705,JCYJ20170302152718747); Research Funding from Shenzhen University (grant no. 2016030); China Postdoctoral Science Foundation (grant nos. 2018M633115); Development and Reform Commission of Shenzhen Municipality Foundation.

References

1. W. J. Bock, J. Chen, P. Mikulic, and T. Eftimov, "A Novel Fiber-Optic Tapered Long-Period Grating Sensor for Pressure Monitoring," IEEE Trans. Instrum. Meas. **56**(4), 1176–1180 (2007).
2. W. J. Bock, J. Chen, P. Mikulic, T. Eftimov, and M. Korwin-Pawlowski, "Pressure sensing using periodically tapered longperiod gratings written in photonic crystal fibres," Meas. Sci. Technol. **18**(10), 3098–3102 (2007).
3. X. Zhong, Y. Wang, C. Liao, S. Liu, J. Tang, and Q. Wang, "Temperature-insensitivity gas pressure sensor based on inflated long period fiber grating inscribed in photonic crystal fiber," Opt. Lett. **40**(8), 1791–1794 (2015).
4. Y. F. Zhang, C. C. Chan, Y. M. Chan, and P. Zu, "Tilted long period gratings pressure sensing in solid core photonic crystal fibers," IEEE Sens. J. **12**(5), 954–957 (2012).
5. G. Statkiewicz-Barabach, D. Kowal, M. K. Szczurowski, P. Mergo, and W. Urbanczyk, "Hydrostatic pressure

and strain sensitivity of long period grating fabricated in polymer microstructured fiber," IEEE Photonics Technol. Lett. **25**(5), 496–499 (2013).

6. M. Smietana, W. J. Bock, P. Mikulic, and J. Chen, "Tuned pressure sensitivity of dual resonant long-period gratings written in boron co-doped optical fiber," J. Lightwave Technol. **30**(8), 1080–1084 (2012).
7. M. Xu, L. Reekie, Y. Chow, and J. P. Dakin, "optical in-fibre grating high pressure sensor," Electron. Lett. **29**(4), 398–399 (1993).
8. H.-J. Sheng, W.-F. Liu, K.-R. Lin, S.-S. Bor, and M.-Y. Fu, "High-sensitivity temperature-independent differential pressure sensor using fiber Bragg gratings," Opt. Express **16**(20), 16013–16018 (2008).
9. Q. Zhang, N. Liu, T. Fink, H. Li, W. Peng, and M. Han, "Fiber-optic pressure sensor based on π-phase-shifted fiber Bragg grating on side-hole fiber," IEEE Photonics Technol. Lett. **24**(17), 1519–1522 (2012).
10. C. M. Jewart, Q. Wang, J. Canning, D. Grobnic, S. J. Mihailov, and K. P. Chen, "Ultrafast femtosecond-laser-induced fiber Bragg gratings in air-hole microstructured fibers for high-temperature pressure sensing," Opt. Lett. **35**(9), 1443–1445 (2010).
11. T. Chen, R. Chen, C. Jewart, B. Zhang, K. Cook, J. Canning, and K. P. Chen, "Regenerated gratings in air-hole microstructured fibers for high-temperature pressure sensing," Opt. Lett. **36**(18), 3542–3544 (2011).
12. L. Jin, B.-O. Guan, and H. Wei, "Sensitivity characteristics of Fabry-Perot pressure sensors based on hollow-core microstructured fibers," J. Lightwave Technol. **31**(15), 2526–2532 (2013).
13. Y. Yu, X. Chen, Q. Huang, C. Du, S. Ruan, and H. Wei, "Enhancing the pressure sensitivity of a Fabry-Perot interferometer using a simplified hollow-core photonic crystal fiber with a microchannel," Appl. Phys. B **120**(3), 461–467 (2015).
14. Y. Wang, D. N. Wang, C. Wang, and T. Hu, "Compressible fiber optic micro-Fabry-Pérot cavity with ultra-high pressure sensitivity," Opt. Express **21**(12), 14084–14089 (2013).
15. B. Xu, C. Wang, D. N. Wang, Y. Liu, and Y. Li, "Fiber-tip gas pressure sensor based on dual capillaries," Opt. Express **23**(18), 23484–23492 (2015).
16. X. Wang, J. Xu, Y. Zhu, K. L. Cooper, and A. Wang, "All-fused-silica miniature optical fiber tip pressure sensor," Opt. Lett. **31**(7), 885–887 (2006).
17. D. Donlagic and E. Cibula, "All-fiber high-sensitivity pressure sensor with SiO2 diaphragm," Opt. Lett. **30**(16), 2071–2073 (2005).
18. J. Ma, J. Ju, L. Jin, and W. Jin, "A compact fiber-tip micro-cavity sensor for high-pressure measurement," IEEE Photonics Technol. Lett. **23**(21), 1561–1563 (2011).
19. C. Liao, S. Liu, L. Xu, C. Wang, Y. Wang, Z. Li, Q. Wang, and D. N. Wang, "Sub-micron silica diaphragm-based fiber-tip Fabry-Perot interferometer for pressure measurement," Opt. Lett. **39**(10), 2827–2830 (2014).
20. Z. Zhang, C. Liao, J. Tang, Z. Bai, K. Guo, M. Hou, J. He, Y. Wang, S. Liu, F. Zhang, and Y. Wang, "High-Sensitivity Gas-Pressure Sensor Based on Fiber-Tip PVC Diaphragm Fabry-Perot Interferometer," J. Lightwave Technol. **35**(18), 4067–4071 (2017).
21. X. Zang, Y. Jiang, X. Wang, X. Wang, J. Ji, and M. Xue, "Highly sensitive pressure sensors based on conducting polymer-coated paper," Sens. Actuators B Chem. **273**(10), 1195–1201 (2018).
22. F. Guo, T. Fink, M. Han, L. Koester, J. Turner, and J. Huang, "High-sensitivity, high-frequency extrinsic Fabry-Perot interferometric fiber-tip sensor based on a thin silver diaphragm," Opt. Lett. **37**(9), 1505–1507 (2012).
23. F. Xu, D. Ren, X. Shi, C. Li, W. Lu, L. Lu, L. Lu, and B. Yu, "High-sensitivity Fabry-Perot interferometric pressure sensor based on a nanothick silver diaphragm," Opt. Lett. **37**(2), 133–135 (2012).
24. J. Ma, W. Jin, H. L. Ho, and J. Y. Dai, "High-sensitivity fiber-tip pressure sensor with graphene diaphragm," Opt. Lett. **37**(13), 2493–2495 (2012).
25. W. Talataisong, D. N. Wang, R. Chitaree, C. R. Liao, and C. Wang, "Fiber in-line Mach-Zehnder interferometer based on an inner air-cavity for high-pressure sensing," Opt. Lett. **40**(7), 1220–1222 (2015).
26. Z. Li, C. Liao, Y. Wang, L. Xu, D. Wang, X. Dong, S. Liu, Q. Wang, K. Yang, and J. Zhou, "Highly-sensitive gas pressure sensor using twin-core fiber based in-line Mach-Zehnder interferometer," Opt. Express **23**(5), 6673–6678 (2015).
27. M. Deng, C. P. Tang, T. Zhu, Y. J. Rao, L. C. Xu, and M. Han, "Refractive index measurement using photonic crystal fiber-based Fabry-Perot interferometer," Appl. Opt. **49**(9), 1593–1598 (2010).